

# When might we break the rules? A statistical analysis of aesthetics in photographs

Justin Wang<sup>1</sup>, Marie A. Lee<sup>2</sup>, Thomas C. M. Lee<sup>1\*</sup>

**1** Department of Statistics, University of California at Davis, Davis, CA, USA

**2** Department of Art and Graphic Design, University of the Pacific, Stockton, CA, USA

\* tcmlee@ucdavis.edu

## Abstract

High-quality photographs often follow certain high-level rules well known to photographers, but some photographs intentionally break these rules. Doing so is usually a matter of artistry and intuition, and the conditions and patterns that allow for rule-breaks are often not well articulated by photographers. This article first applies statistical techniques to help find and evaluate rule-breaking photographs, and then from these photographs discover those patterns that justify their rule-breaking. With this approach, this article discovered some significant patterns that explain why some high-quality photographs successfully break the common photographic rules by positioning the subject in the center or the horizon in the vertical center. These patterns included reflections, leading lines, crossing objects, ambiguous lines, implied lines, thirds line subjects, and busy foregrounds for center horizon photographs, and symmetry, circular-shaped objects, thirds line elements, gestalt, framing, leading lines, and perspective lines for center subject photographs.

## Introduction

High-quality photographs, like other artworks, often adhere to a set of design principles agreed upon by photographers. There are six fundamental principles of design: line, shape, space, texture, light, and color [1]. Applying such principles leads to well-known rules in photography, such as the rule of thirds [2] and the rule of odds [3]. Some high-quality photographs deliberately do not possess the desirable features present in most photographs, purposefully violating photographic design principles and rules. They “break the rules,” so to speak. The breaking of the rules is usually based on feel and intuition, as opposed to relying on specific patterns of conditions to hold. We aimed to solidify concrete conditions and patterns under which the breaking of some of the most well-known photographic rules may occur. To do this, we used a quantitative approach based on statistical and image processing techniques to identify and analyze high-quality rule-breaking photographs.

Our work is closely related to aesthetic quality classification. Aesthetic quality classification, a subfield of computer vision, applies classification models and feature construction to automatically differentiate higher quality photographs from lesser quality ones. Two of the most influential early works in the field were [4] and [5]. Both approached the problem by generating a set of features based on properties of photographs and then performing classification on this set of features. A total of 52 candidate features were presented by [4] that made some level of intuitive sense. They

then fit a classification model with all of the candidate features, and finally performed  
model selection, retaining the 15 most “important” features. The authors of [5]  
interviewed professional photographers to figure out what properties they believed  
comprised a good photograph. Based on the interviews, they came up with six features  
to approximate the properties described by the photographers.

Works following [4] and [5] aimed to improve the quality of the features used to  
perform the classification. The authors of [6] first extracted the subject region from a  
photograph, and then devised features that take advantage of the ability to isolate the  
subject, such as lighting contrast between subject and background, and color simplicity  
of the background. The authors of [7], [8], and [9] constructed features based on  
high-level describable attributes such as whether an animal is present in the photograph.  
A model with features all based on color harmony was proposed by [10], while a  
low-level feature approach was proposed by [11], in which most of the features did not  
correspond to describable attributes or photographic intuition.

Recent works in this field abandon the features approach and use deep learning  
models, specifically deep convolutional neural networks (DCNNs), to classify the  
photographs and their pixels directly without using features as an intermediate. Such  
works include [12], [13] and [14]. Such approaches achieve a lower classification error,  
and thus higher predictive power than the past feature-based approaches. However, they  
come at the cost of being much less interpretable than the feature-based approach, as in  
general, there is no simple way to map features automatically produced by DCNNs to  
high level features interpretable by humans.

## Overview of our work

Here we provide an overview of our analysis, which will follow much more closely to the  
features-based approach, as interpretability of the features is crucial to our analysis.  
Our features will be high-level and describable, and will correspond to what can be  
observed in a photograph by the human eye.

We will use the AVA dataset (more below) in our study. Every photograph in this  
dataset comes with a rating, from 1 to 10. We shall begin with calculating a set of  
numerical features for all the photographs in the dataset. We will then use these  
numerical features, together with the photographs’ corresponding ratings, to fit a  
statistically interpretable classifier. From this, we will identify a set of features that are  
statistically significant for predicting the ratings. These features are useful tools in  
analyzing the rule-breaking photographs.

Next, we will review a small, random sample of the dataset and develop a  
human-guided automatic algorithm that will be applied to the whole dataset. It will  
enable us to identify a set of features (or patterns) that may be related to rule-breaking.

Lastly, we will study and compare those statistically significant features from the  
classifiers with those from the human-guided algorithm, and obtain our paper’s main  
results: examples of rule-breaking in photography; see Fig 1 for a flowchart  
summarizing the above steps.

We will focus on identifying and analyzing high-quality photographs that violate two  
specific important photographic rules. The first rule is that photographs with a visible  
horizon should not place the horizon right in the center of the photograph. Throughout  
the paper, we will refer to high-quality photographs that violate this rule as “center  
horizon photographs”. The second rule is that photographs containing a subject should  
not place the subject in the center of the photograph. We will refer to high-quality  
photographs that violate this rule as “center subject photographs.”

As we do not have the permission to re-publish the AVA photographs in this journal,  
we refer the reader to <https://github.com/thomascmlee/rulebreaking> for those

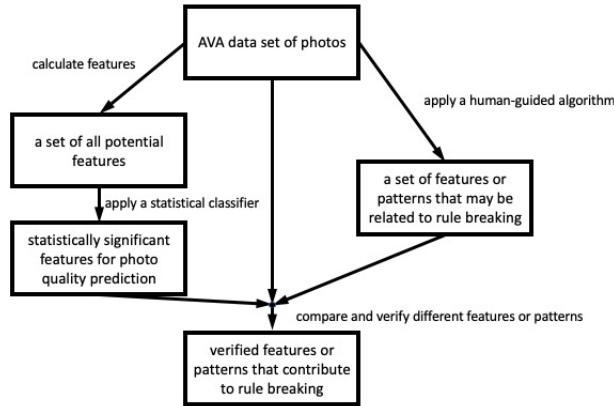


**Fig 1. A flowchart summarizing the analysis of the paper.**

photographs we reference below. These photographs are referenced as Fig OS1, Fig OS2, and so on, where "OS" stands for online-supplement.

## Background and preliminaries

Here we will briefly discuss the HSV color model, which we have used in many of our features. Additionally, many of our features were based on the preliminary steps of subject region extraction and the named color histogram, which we also describe below.

### HSV color model

The HSV color model is an alternate representation of the standard RGB model, which models each pixel of an image as a mixture of red, blue, and green [15]. Under the HSV color model, images are modeled as a collection of 3 matrices - H, S, and V, each of size  $n \times m$ , where  $n$  and  $m$  represent, respectively, the height and width in pixels of the image. The  $H$ , or hue matrix represents the overall color of each pixel along a circular color spectrum. Corresponding to a circle of colors, values in the hue matrix are integers that range from 0 to 360. Fig OS1 shows the full wheel of colors represented in the hue matrix, as described in The Colorist [16]. The  $S$ , or saturation matrix represents how saturated or "pure" the color of each pixel is. The values in the  $S$  matrix range from 0 to 100, with 100 being the most saturated. The  $V$ , or value matrix represents the brightness of each pixel, and the values also range from 0 to 100, with 100 being the brightest. The elements in each of the three matrices are often standardized to fall in the range  $[0, 1]$ .

### Saliency map

Two of our features require that the region occupied by the subject, or at the very least important objects, be extracted and identified from photographs. These features are the percentage area occupied by the subject and the lighting contrast between subject and background. To extract the subject region, we used the algorithm Robust Background Detection [17] to obtain what is known as a saliency map. A saliency map is a simplified representation of an image that highlights its salient, or important areas [18]. Our resulting saliency map from Robust Background Detection is an image represented by a  $n \times m$  matrix of pixel values ranging from 0 to 255, with 255 being the brightest

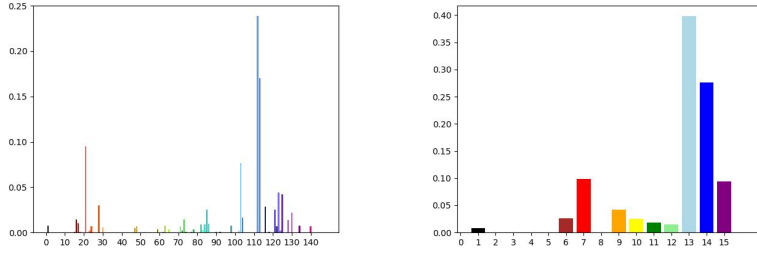


**Fig 2. Named colors histogram and a condensed version.**

value. Bright pixel values in a saliency map correspond to important regions in an image (generally the subject itself).

For our two features that require the saliency map, we only need a binary representation. In other words, we only need a representation that identifies whether any given pixel belongs to the subject region. The most straightforward way to binarize a saliency map is to choose a threshold  $t \in \mathbb{Z}$ , such that a given pixel's binary representation is 1 if the pixel value in the original saliency map exceeds  $t$ , and 0 if it is less than or equal to  $t$ . From experimentation, we found that  $t = 100$  was a good choice. An example saliency map and its binarization are shown in Fig OS2.

### Named color histogram

In image processing, a color histogram is a way to represent the distribution of colors in an image [19]. When constructing a color histogram, the image usually is represented in RGB color space and the  $R$ ,  $G$ , and  $B$  matrices are each quantized into bins of size  $N$ . Each pixel of the image is then assigned to one of  $N^3$  bins, producing a histogram with  $N^3$  bins. Color histograms are a useful tool, but they are not very interpretable at a high level, particularly as a visualization of the colors featured in an image because the resulting bins do not correspond well to the colors known to the human eye. Since we would like to identify high-level patterns among images, we used a modified approach to the color histogram that uses recognizable, or named, colors. We shall call our modified approach the named color histogram.

For our named colors, we used the standard 140 web colors [20]. These are the standard colors used in modern web browsers, and taken together, cover a comprehensive and diverse range of colors. We obtained the coordinate representation in HSV space for each of the 140 colors. To produce a named color histogram for a given photograph, one could then compute the euclidean distance of every pixel in the photograph to each of the 140 named colors, and then assign each pixel to the closest named color. In practice, however, the strategy mentioned above proved to be time inefficient. To speed up the process, we used 8 x 8 non-overlapping sliding windows, averaging the pixel values in each window. We show an example of a named color histogram in Fig 2. In the figure we also provide a condensed histogram which merges similar colors into the same color family. It results in a display of only 16 of the most common named colors.

## Feature description

132

### Average value and saturation

133

We start with some simple features: the average value and saturation of each image. High-quality images tend to have a lower value (less bright) and are more saturated (purer in color) than low-quality images. To obtain the average value and saturation of a given photograph, one can simply average all of the values in the  $V$  and  $S$  matrices, respectively. More precisely, the average value feature  $av$  and average saturation feature  $as$  are given, respectively, by

$$av = \frac{1}{nm} \sum_{i=1}^n \sum_{j=1}^m v(i, j) \quad \text{and} \quad as = \frac{1}{nm} \sum_{i=1}^n \sum_{j=1}^m s(i, j),$$

where  $v(i, j)$  and  $s(i, j)$  represent the  $(i, j)^{\text{th}}$  element of matrices  $V$  and  $S$ , respectively, and  $n$  and  $m$  represent respectively the height and width in pixels of the photograph. Note that we are not using average hue as a feature, as it does not make much sense to average all the colors in the color spectrum of the pixels.

140

141

142

143

### Clarity

144

One of the most important defining features of high-quality photographs is clarity. High-quality photographs are generally very clear and in-focus, and look very “crisp,” whereas low-quality photographs are often grainy, blurry, and out of focus. We used the clarity feature from [5], which we found to be quite effective.

145

146

147

148

To define this measure, consider the HSV representation of an image. Let  $F$  represent the two dimensional Fast Fourier transform of the  $V$  matrix. Let  $C = \{(u, v) : F(u, v) > \epsilon\}$ , where  $\epsilon$  is a prefixed threshold. Similar to [5], we chose  $\epsilon = 5$ . Our clarity feature  $cf$  is defined as follows:

$$cf = \frac{\|C\|}{\|F\|}.$$

In other words,  $cf$  represents the percentage of high-frequency elements in  $F$ . Fig OS3 gives two examples of photographs with their clarity measures. The photograph on the left is much clearer than the photograph on the right and thus has a much higher clarity measure.

149

150

151

152

### Size and aspect

153

Two simple but very effective features included in our model are size and aspect. High-quality photographs tend to be considerably larger than average than low-quality ones. They also tend to be more concentrated in specific aspect ratios when comparing to low-quality photographs.

154

155

156

157

Our size feature for a given image is simply  $S = mn$ , where  $n$  and  $m$  represent the pixel height and width of the image, respectively. The aspect ratio feature is  $A = m/n$ , the width divided by the height. When we construct our model, we will turn aspect ratio into a categorical variable, with its categories defined by aspect ratio ranges.

158

159

160

161

### Hue count

162

In the HSV color model, the hue represents actual color identity, whereas saturation and value represent the “pureness” and brightness of that color, respectively. By adjusting the saturation and value, one can obtain a very different “looking” color even when the

hue is kept unchanged. Often high-quality photographs do not contain that many different hues. Instead, they vary greatly in saturation and value, resulting in a photograph that appears very rich in color despite the lack of many unique hues. The notable exceptions to this principle are high-quality images that are deliberately colorful, which will indeed have high hue counts. In contrast, low-quality photographs, which often do not have a clear focus, will often have a high hue count. These many different hues are represented in the many different colored objects that are often present in low-quality photographs.

We used the hue count feature from [5]. The idea of this measure is to group the hues of every pixel in a photograph into bins and then count how many of these bins exceed a certain threshold. We divided the overall hue range into 20 bins, each of size 18. Pixels with a value less than 0.15 or greater than 0.95, and pixels with saturation less than 0.2 were discarded before binning. The reason to do this is that any pixel with a value less than 0.15 will effectively appear black, and any pixel with a value greater than 0.95 will effectively appear white, regardless of its actual hue. Pixels with saturation less than 0.2 generally appear as some shade of grey, no matter the hue.

After discarding some pixels as described above, we grouped each remaining pixel into its appropriate hue bin, and constructed a hue histogram with 20 total bins. Let  $M$  represent the largest bin count among all 20 bins, and let  $\alpha$  be a small number between 0 and 1. For our hue count feature we used  $\alpha = 0.05$ . Our hue count feature  $HC$  is defined as follows:

$$HC = \# \text{ bins with bin count greater than } \alpha M.$$

Fig OS4 gives two examples of photographs with their hue count measures. The photograph on the left is much more focused in colors than the photograph on the right, a fact that is reflected by its lower hue count.

## Color nearest neighbors

We devised a measure to assess whether a given photograph more closely resembles a high-quality photograph or a low-quality photograph, in terms of the colors present in the photograph. Using the color histograms of the photographs, we define a color distance measure between two photographs  $P_1$  and  $P_2$  as follows:

$$cd = \sum_{i=1}^B (h_{i1} - h_{i2})^2,$$

where  $B = 140$  represents the total number of bins in the color histogram, and  $h_{ij}$ ,  $j = 1, 2$  represents the frequency of the  $i^{th}$  bin in photograph  $P_j$ . Using this distance measure, we compute the  $K$  nearest neighbors for each photograph using  $cd$ . Then our color nearest neighbors feature  $pc$  is the proportion of these  $K$  nearest neighbors that are high-quality photographs:

$$pc = \frac{1}{K} \sum_{i=1}^K \mathbf{I}(N_i \text{ is a high-quality photograph}),$$

where  $N_i$ ,  $i = 1, \dots, 20$  represents the  $i^{th}$  nearest neighbor, and  $\mathbf{I}(\cdot)$  is the indicator function. For our color nearest neighbors feature, we chose  $K = 20$ . Fig OS5 shows a photograph with 3 of its 20 nearest neighbors.

## Percentage area of subject

For this feature, we measure the total area percentage of the photograph taken up by the subject and/or prominent objects in the photograph. To do so, we use the binary

saliency map  $B$  and compute the percentage area as follows:

$$pa = \frac{1}{nm} \sum_{i,j} B(i,j),$$

where  $n$  and  $m$  represent the height and width of  $B$ , respectively, and  $B(i,j)$  represents the  $(i,j)^{\text{th}}$  pixel of  $B$ . Fig OS6 gives an example of two photographs with their respective percentage area measures.

## Lighting contrast

One commonly known principle in photography is to make the subject stand out from its background. In high-quality photographs, this often translates to the subject being distinctly brighter than the background. We adapted the lighting contrast measure from [6] to measure the contrast between subject and background. To measure the contrast in lighting between the subject and the background, we used the binary saliency map  $B$  and the brightness matrix  $V$ . While we used the same feature definition as [6], we used a much more powerful saliency map to detect the subject, which resulted in our lighting contrast measure being much stronger than their version.

We first define  $L_s$  and  $L_b$ , the average lighting within the subject region and background region, respectively:

$$L_s = \frac{1}{n_s} \sum_{i,j} V(i,j) \mathbf{I}(B(i,j) = 1) \quad \text{and} \quad L_b = \frac{1}{n_b} \sum_{i,j} V(i,j) \mathbf{I}(B(i,j) = 0),$$

where  $n_s$  and  $n_b$  represent the number of elements in  $B$  that are 1 and 0, respectively, and  $\mathbf{I}(\cdot)$  is the indicator function. The lighting contrast is then defined as:

$$lc = \log \left( \frac{L_s}{L_b} \right).$$

We take the logarithm to prevent the lighting contrast measure from getting extremely small or large. This issue often arises when the background is completely black or white, which leads to extreme values if the logarithm is not taken. Fig OS7 gives examples of two photographs with their respective lighting contrast measures. The photograph on the left has a much greater lighting contrast between the subject and the background than the photograph on the right, and therefore has a much larger lighting contrast measure.

## The AVA dataset

Our work used the AVA dataset [21] for both our high-quality and low-quality photographs. AVA consists of 255,508 photographs submitted to DPChallenge.com, a photography contest website. Every photograph uploaded to DPChallenge is submitted to a specifically themed "challenge," with many diverse themes such as "Plants in B/W," "The Nature of Time," and "Light Study." There are a total of 1,447 challenges represented among all of the photographs in AVA. Every photograph on DPChallenge was given a 1-10 rating by any other registered user with 10 being the highest. AVA provides, for every photograph in the dataset, a count of the number of users who gave the photograph each of the 10 possible numerical ratings. The number of ratings given to each photograph ranges from 78 to 549, with a mean of 210 ratings given. In order to create specific datasets of high and low-quality photographs, we averaged the rating of every photograph in the dataset and then respectively took the top 5% and bottom 5%

of all photographs in AVA in terms of average rating. The resulting high and  
222  
low-quality datasets each contain 12,777 photographs. In Fig OS8 we show some  
223  
examples of photographs belonging to both the high and low-quality datasets. The AVA  
224  
dataset can be obtained from  
225  
[https://github.com/mtobeiyf/ava\\_downloader/tree/master/AVA\\_dataset](https://github.com/mtobeiyf/ava_downloader/tree/master/AVA_dataset).  
226

## Justifying the use of AVA

Since its creation in 2012, AVA has emerged as the preeminent dataset used in  
228  
aesthetics quality classification. It is by far the largest publicly available dataset of  
229  
photographs with aesthetic labels. Many researchers in the field use AVA as their main  
230  
dataset to evaluate their methodology [12, 14, 22]. While we are using many of the same  
231  
methodology as in aesthetics quality classification, our primary goal is to analyze  
232  
rule-breaking high-quality photographs. This raises the natural question of whether  
233  
AVA is suited for this purpose. We will address three potential concerns with using the  
234  
AVA dataset for our analysis.  
235

The first potential concern is whether user ratings on a website is an accurate  
236  
measure for objective quality for a given photograph compared to, for example, a panel  
237  
of photography experts. According to [21], each photograph in the dataset received at  
238  
least 78 ratings, with the average number of ratings being 210. This indicates that the  
239  
average rating for each photograph is reasonably aggregated, and is not among a small  
240  
number of people, which would be subject to high variance. In addition, DPChallenge  
241  
requires registration in order to rate images, and one would expect at least a base level  
242  
of interest and knowledge on a user's involvement to rate photographs. Finally, in  
243  
observing the high-quality dataset that we obtained, we have found the photographs in  
244  
the dataset to indeed be of high quality.  
245

The second potential concern is whether the average rating of a photograph  
246  
accurately captures the entire distribution of ratings. After all, a controversial  
247  
photograph with many low ratings as well as many high ratings could well end up with  
248  
a similar score to a photograph with mostly average ratings. This issue is addressed  
249  
in [21], and they write that the score distributions are well approximated by Gaussian,  
250  
with a root mean square error less than 0.06. Overall, it appears that the vast majority  
251  
of photographs have a consensus in scores.  
252

The third potential concern is whether AVA represents a good sample of all  
253  
photographs in general, given that it is comprised of samples of themed challenges.  
254  
Every photograph belonging to the same themed challenge will not be independent of  
255  
one another. There are 1,447 themed challenges represented among the photographs in  
256  
the data, and they cover a wide variety of themes. This means that there is roughly an  
257  
average of 177 photographs per themed challenge. Looking at the challenges themselves,  
258  
they cover a vast variety of themes and topics in photography. With this many  
259  
challenges represented in the dataset, it can be safely assumed that a wide breadth of  
260  
types of photography are represented. Looking through the high-quality photographs, it  
261  
was clear that there is a large diversity of types of photographs.  
262

## Cleaning, analyzing, and modeling the data

We now describe the details of the data cleaning and modeling process. We also present  
264  
our results from the data analysis and classification.  
265

## Creating and cleaning the data

We had nine features altogether, and they were all implemented as described in Section **Feature description**. Two of them, percentage area of subject and lighting contrast, were based on the saliency map described in Section **Saliency map**. The color nearest neighbors was based on the named color histogram described in Section **Named color histogram**. We were unable to process a tiny fraction of photographs among both the high and low-quality datasets (less than 0.001% for each dataset). The final features dataset for high and low-quality photographs were of dimension 12,766 x 9 and 12,762 x 9, respectively.

Photographs without clear subjects often confused the Robust Background Detection algorithm we used to construct our saliency map. The resulting saliency map would often contain a large majority of values that were equal to or close to 255. We found that photographs whose percentage area of the subject measure was greater than 0.7 almost always had this problem. For such photographs it would not be useful to measure any of the features based on the saliency map. We identified 383 high-quality photographs and 169 low-quality photographs that had a percentage area of subject exceeding 0.7. To minimize the impact of these photographs on the classification results, we imputed the mean of the remaining high-quality and low-quality photographs respectively for each of these three features. Fig OS9 shows an example of a high-quality photograph lacking a subject that confused the subject region extraction algorithm.

The aspect ratio feature was split into categories and converted to a categorical variable via the creation of several dummy variables. There are standard aspect ratios that photographs often adhere to, and we found that most photographs could be classified as being at or close to one of these standard aspect ratios. We ended up creating six categories for aspect ratio: Tall, 3:4, Square, 4:3, 3:2, and Wide based on cutoff ranges for the numerical aspect ratio value. More details about the specific cutoffs we used to construct these categories can be found in the next subsection.

## Feature comparison between high and low quality datasets

To better understand the high-quality photographs in our data and properties of high-quality photographs in general, we performed some rudimentary data analysis on our high-quality dataset. We first converted the value of every feature in both the high and low-quality datasets into their percentile scores. For example, if the percentile of the value of a particular feature in a photograph is 0.7, it means that this photograph has a greater value for this particular feature than 70% of the rest of the data (among both the high and low-quality datasets). We compute 99% confidence intervals for the mean difference in percentile between the high and low-quality datasets for each feature in Table 1. Below we discuss the confidence interval for each feature and the reasoning behind their values:

- *Avg. value.* With high confidence, the mean percentile of average value among high-quality photographs is between 3.7% and 5.6% lower than that of low-quality photographs. The high-quality dataset contains a significant subset of photographs that feature a lot of black colors, such as photographs taken in nighttime and objects on black backgrounds. This subset of photographs lowers the average value (brightness) within the high-quality dataset.
- *Avg. Saturation.* With high confidence, the mean percentile of average saturation among high-quality photographs is between 0.5% and 2.4% higher than that of low-quality photographs. The high-quality dataset features many photographs that are generally richer and deeper in color, while low-quality photographs tend to be fainter in color.

**Table 1.** Confidence intervals of the difference between high and low-quality datasets for each feature.

Feature	Lower Bound	Upper Bound
Avg. Value	-0.056	-0.037
Avg. Saturation	0.005	0.024
Clarity	0.266	0.283
Size	0.199	0.28
Hue Count	-0.099	-0.081
Color Nearest Neighbors	0.166	0.184
Percentage Area	-0.024	-0.009
Lighting Contrast	0.061	0.076

- *Clarity.* With high confidence, the mean percentile of clarity measurement among high-quality photographs is between 26.6% and 28.3% higher than that of low-quality photographs. A higher clarity measure of a photograph implies greater clarity, so this is an unsurprising outcome. Low-quality photographs are frequently blurry and unfocused, and high-quality photographs are generally crisp and focused. Some number of high-quality photographs are blurry and thus have a low clarity measure. However, such photographs are not that common, and they tend to be blurry on purpose. The reasons for blurriness among high-quality photographs were usually things like fog and motion.
- *Size.* With high confidence, the mean percentile of size among the high-quality dataset is between 19.9% and 28% higher than that of low-quality photographs. We found high-quality photographs to be considerably larger on average than low-quality photographs. Low-quality photographs are often taken with poor equipment (e.g., camera phones), and thus tend to be smaller.
- *Hue count.* With high confidence, the mean percentile of hue count among the high-quality dataset is between 8.1% and 9.9% lower than that of low-quality photographs. Low-quality photographs are often “messy” in color, as they often contain a random assortment of objects with all types of different hues. High-quality photographs are more focused, which often leads to having a lower number of actual hues.
- *Color nearest neighbors.* With high confidence, the mean percentile of size among high-quality photographs is between 16.6% and 18.4% higher than that of low-quality photographs. Since this feature measures the percentage of the  $K = 20$  nearest color neighbors of a given photograph that are high-quality, it makes sense that a high-quality photograph would, on average, have more nearest color neighbors that are also of high-quality. This indicates that high-quality photographs are more likely to resemble one another in terms of color distribution, and similarly for low-quality photographs.
- *Percentage area.* With high confidence, the mean percentile of percentage area among high-quality photographs is between 0.9% and 2.4% lower than that of low-quality photographs. While the difference is only slight, it is nevertheless significant. High-quality photographs are generally careful about the amount of photograph area the subject takes up, and having the subject take up a large amount of area is a deliberate choice. On the other hand, low-quality photographs often are snapshots of people or objects taken quite carelessly, and the result is that the subject often takes up more area.

### Aspect - High Quality vs. Low Quality

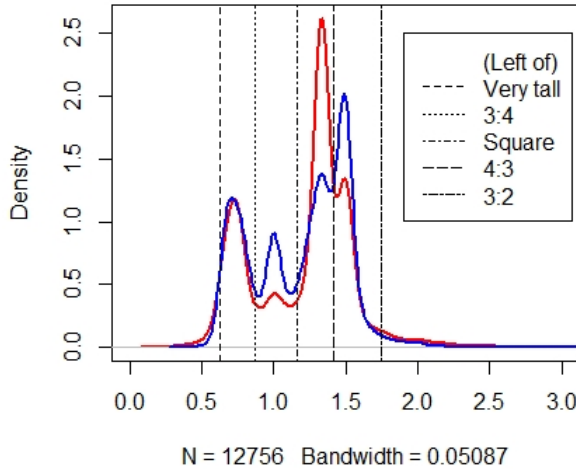


**Fig 3. Comparing the distribution of aspect ratio between the high-quality (blue) and low-quality (red) photographs.**

- *Light contrast.* With high confidence, the mean percentile of light contrast among high-quality photographs is between 6.1% and 7.6% higher than that of low-quality photographs. Contrast in lighting between subject and background is a feature of a good photograph. It is something high-quality photographs often possess and low-quality photographs often lack.

To better understand the differences in aspect ratio between high and low-quality photographs, we constructed kernel density plots for the distributions of aspect ratio between high and low-quality photographs in Fig 3. We used a bandwidth of 0.05087 for the plot. The density of high-quality photographs is represented in blue, and the low-quality in red. We grouped the kernel density plot into range categories corresponding to the six aspect ratio categories we created, as depicted in Fig 3. In the legend, a category name that appears next to a given dotted line is the category that comprises the range to the left of that dotted line (but to the right of the previous dotted line, if applicable). For instance, the range between the first and second lines corresponds to a 3:4 aspect ratio. From the figure, we see that there are more low-quality photographs with a 4:3 aspect ratio, but more high-quality photographs with Square and 3:2 aspect ratios. We believe the reason for this is that the 4:3 aspect ratio is the default ratio setting in most non-professional cameras, and thus low-quality photographs, which are often taken with much less care, often just stick to the default ratio. On the other hand, high-quality photographs are a lot more likely to be experimental with different aspect ratios.

#### Subcategories

When looking at different categories of photographs, certain design principles and features are more important than others. For example, a photograph of a subject in a completely black background will invariably have the average brightness greatly lowered by the background. Thus, it would be more useful for such photographs to measure the average brightness of the subject instead. Below we describe four subcategories of

high-quality photographs we labeled to supplement our analysis. We obtained each  
subcategory described through a mix of computational methods and manual labeling of  
the high-quality photographs. For each candidate photograph and each subcategory, we  
labeled the photograph 1 if it fell into that subcategory, and 0 otherwise.

- *Silhouettes*. A silhouette is the image of a person, animal, object, or scene  
represented as a solid shape of a single color, usually black, with its edges  
matching the outline of the subject. They often have a sunrise or sunset in the  
background and are therefore intensely orange in color, although this is not always  
the case. Through manual labeling, we identified a total of 842 silhouettes among  
all of the high-quality photographs. Fig OS10 gives some examples of silhouettes.
- *Landscapes*. We define landscapes as photographs featuring a horizon line, or in  
which the horizon is at least visible, even if it is not visible as a physical line. The  
landscape designation will be important in identifying one of our rule-breaks,  
center horizon. We identified 2902 landscapes among the high-quality  
photographs through manual labeling. Fig OS11 shows some examples of  
landscape photographs.
- *Monochrome Background*. We use this designation to refer to photographs that  
contain a subject with a background of completely one color. We further  
subdivided this category into six subcategories based on the color of the  
background. They were as follows: black, white, blue, gray, green, and other. The  
last category, other, consisted of background colors that did not appear frequently  
enough to warrant their own category. To obtain monochrome background  
photographs, we used the saliency map to isolate the background for every  
photograph in our high-quality data. We then computed the color histogram on  
the background only. To do this, we used the condensed color histogram  
mentioned in Section **Named color histogram**, as it provided more precise  
measurements. We considered a photograph that appeared in more than 90% of a  
particular color to have that color as a background (occasionally stray colors were  
picked up slightly in this process, but they had a minimal effect on the final  
result). We identified a total of 1916 monochrome background photographs among  
the high-quality dataset. Fig OS12 shows some examples of monochrome  
background photographs with various background colors.
- *Black and White*. As the name suggests, black and white photographs lack color,  
and rely only on black, white, and varying shades of grey. From a computational  
perspective, the  $H$  and  $S$  matrices are completely zero for black and white  
photographs, and thus the only valued matrix is  $V$ . Equivalently, the  $H$  and  $S$   
matrices are completely zero if and only if the hue count feature is 0. Thus we  
obtained black and white high-quality photographs simply by identifying the  
high-quality photographs that had a hue count value of 0. We identified a total of  
1201 black and white photographs within the high-quality data.

## Classification results

We used two classifiers: logistic regression [23] and random forest [24]. Logistic  
regression is a linear classifier and is highly interpretable, as the direction for the  
coefficient each feature is clearly specified. If we are willing to put parametric  
assumptions on the error then we are also able to compute a  $p$ -value for the coefficient  
of each feature. Random forest, while less interpretable, is a far more powerful and  
sophisticated classifier that generally performs better than logistic regression. For  
logistic regression, we chose 0.5 as the cutoff for predicted probabilities: high-quality if

**Table 2.** Confusion matrix for logistic regression.

	Predicted Low	Predicted High	Total
Actual Low	10103	2659	12762
Actual High	3165	9601	12766
Total	13268	12260	25528

**Table 3.** Confusion matrix for random forest.

	Predicted Low	Predicted High	Total
Actual Low	10538	2224	12762
Actual High	3323	9443	12766
Total	13861	11667	25528

exceeding the cutoff, and low-quality otherwise. For random forest, we used 500 bootstrapped trees and three randomly sampled candidate features at each node split.

We used 5-fold cross-validation and averaged the classification error on the test set from each fold. We found these cross-validated classification errors to be 0.2281 and 0.2173 for logistic regression and random forest, respectively. For logistic regression, noted both the direction and *p*-value of the coefficient of each feature. For each of our 9 features, both the direction and significance matched the results provided in the confidence intervals reported in Table 1.

We present the confusion matrix using the cross-validated predictions for both logistic regression and random forest in Table 2 and Table 3, respectively. Most notably, the false positive rates are 0.208 and 0.174, while the false negative rates are 0.248 and 0.26, for logistic regression and random forest, respectively. This indicates that for both classifiers, high-quality photographs are more likely to be misclassified as low-quality photographs than the other way around. This is due to low-quality photographs being generally more homogeneous in their feature directions, e.g., they are generally more blurry, have a higher hue count, and higher saturation. While exceptions certainly exist among low-quality photographs, their feature measurements are more often as expected. On the other hand, high-quality photographs have a much broader diversity in feature measurements. For example, a foggy photograph and a colorful photograph will score ‘poorly’ in the blur and hue count features, respectively, but for a good reason. We also note that logistic regression is less likely to misclassify a high-quality photograph as being of low-quality, but more likely to misclassify a low-quality photograph as being of high-quality.

We also present the precision-recall curves for both classifiers in Fig 4. It appears that for recall range from 0 to 0.4, logistic regression has higher precision, and for recall range from about 0.5 to 0.9, random forest has higher precision. At recall 0.5, they appear to have about the same precision. The precision and recall associated with our actual logistic regression predictions are 0.783 and 0.752. The precision and recall associated with our actual random forest predictions are 0.809 and 0.74, respectively.

## Analyzing photographic rule-breaks

We identified two specific important photographic rule-breaks found among high-quality photographs. The first is found among landscape photographs and it states that the horizon line should not be placed at the halfway point/center of the photograph. The

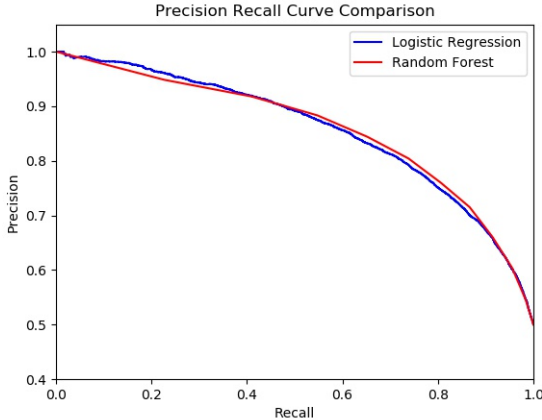


**Fig 4. Precision-recall curves for random forest and logistic regression.**

second is found among photographs containing a subject and it states that the subject should not be placed at the center of the photograph. Both rules are commonly taught to the beginning or intermediate photographers as examples to avoid. However, highly skilled photographers will occasionally choose to break these rules on purpose in their photographs. Traditionally, such rule-breaks are based more on intuition rather than well-specified conditions that allow for breaking the rule. In the following sections, we will explore both rule-breaks computationally using our high-quality dataset, in order to identify common patterns that explain the rule-breaks. We shall refer to these patterns as *explanatory patterns*.

## Horizon lines

Out of 2902 landscape photographs we identified 307, or 10.6% as having placed the horizon line either precisely at or very close to the center of the photograph. For brevity, we will refer to these photographs as *center horizon photographs*. We identified center horizon photographs among all landscape photographs using the following process:

1. We first used an online machine learning API to estimate the position of the horizon line for a given input landscape photograph. The API consists of a convolutional neural network that was trained on a large number of photographs containing horizon lines. The output was a set of two 2D coordinates, one for each endpoint of the estimated horizon line. In the vast majority of cases, the  $y$ -coordinate of the two endpoints were the same or very close to being the same, causing the estimated horizon to be a straight or near-straight line.
2. To obtain our horizon line estimate, we averaged the  $y$ -coordinates of the two endpoints, and then transformed the result to a real number between 0 and 1. This real number represents the relative position of the horizon line in relation to the photograph's height, with 0 being at exactly the bottom of the photograph, 0.5 being exactly in the middle, and 1 being at exactly the top.
3. Due to truncation errors or some other reasons, occasionally the results obtained from the previous step were not precise. Therefore we performed manual adjustment on the horizon line positions of every landscape photograph to ensure accuracy.

4. After the manual adjustment, we isolated every landscape photograph whose  
489 position estimate was between 0.475 and 0.525 and identified them as center  
490 horizon photographs.  
491

After obtaining the set of center horizon photographs, we then carefully examined  
492 each of them from an artistic point of view, in order to identify explanatory patterns  
493 among them. Specifically, we were interested in compositional devices of photographic  
494 composition, such that removing these devices would cause the photograph to look  
495 strange. Below we describe the eight compositional devices that we identified as the  
496 explanatory patterns that justify why these photographs were able to have the horizon  
497 line placed in the center.  
498

1. *Reflections across the horizon line (“Reflections”)*. Reflections were one of the  
499 most common explanatory pattern we found among center horizon photographs.  
500 We provide some examples of center horizon photographs featuring reflections in  
501 Fig OS13. Such photographs feature objects reflected across the centered horizon  
502 line, almost always over a body of water. Reflections create a symmetry and  
503 balance among the top and bottom halves of the photograph, and as such,  
504 circumvent the horizon line rule. Reflections are compelling enough on their own  
505 that no other explanatory element is generally needed.  
506
2. *Leading lines*. Leading lines are lines in a photograph that lead the eyes to a  
507 particular area [1]. Fig OS14 gives some examples of center horizon photographs  
508 featuring leading lines. Leading lines generally come in the form of bridges and  
509 walkways among the center horizon photographs. They provide depth to the  
510 photograph that allows for the viewer to see it in a more three dimensional  
511 perspective. This has the effect of mitigating the view of seeing the photograph as  
512 “two halves.”  
513
3. *One or more objects “cross” the horizon line (“Object Crossing”)*. Objects  
514 crossings were another one of the most common explanatory patterns that we  
515 found among center horizon photographs, after reflections. It refers to having an  
516 object or several objects in the center horizon photograph “cross over” the  
517 centered horizon line. Fig OS15 gives some examples. Object crossing has the  
518 effect of bridging the top and bottom halves of the photograph, so that they no  
519 longer appear to be two separate halves.  
520
4. *Horizon line is at least somewhat ambiguous (“Ambiguous Line”)*. In some center  
521 horizon photographs, the horizon line exists, but is not particularly well defined.  
522 Fig OS16 provides some examples. In such photographs, there is much less of a  
523 view of a separate top and bottom halves, since their boundary is not quite  
524 noticeable or well defined.  
525
5. *There is another implied line or shapes somewhere else (“Implied Line”)*. Related  
526 to the ambiguity of the horizon line is the notion that there is an implied dividing  
527 line other than the horizon line elsewhere in the photograph. This also includes  
528 shapes formed by elements such as mountain or forest that appear to create  
529 somewhat of a line. Fig OS17 provides some examples of center horizon  
530 photographs in which the horizon line is well-defined, but there is another dividing  
531 line present in the photograph. When another dividing line not located in the  
532 center is present, it breaks the view of a separate top and bottom half.  
533
6. *A subject located on a thirds line (“Thirds Line Subject”)*. The rule of thirds is a  
534 well-known compositional device that states that important compositional  
535 elements of a photograph should generally be placed at thirds intersection points.  
536

**Table 4.** Counts for the center horizon patterns.

Pattern	Count	Exclusive Count
Leading Lines	72	4
Object Crossing	95	7
Ambiguous Line	25	0
Implied Line	51	2
Thirds Line Subject	51	0
Busy Foreground	37	3
Sun	32	1

The rule of thirds is “applied by dividing a medium into thirds both vertically and horizontally, creating an invisible grid of nine rectangles and four intersections” [2]. Some center horizon photographs have a subject, often the main or only subject, located at or near one of the vertical thirds dividing line. Fig OS18 provides two examples of such photographs. This element has the effect of providing a thirds balance horizontally, which mitigates the effect of having a top and bottom half.

- 7. *There is a “busy” foreground that distracts from the horizon line (“Busy Foreground”).* In some center horizon photographs, the bottom half, which represents the foreground of the photograph, commands attention. Fig OS19 provides examples of center horizon photographs with busy foregrounds. Having a busy foreground brings the attention away from the center horizon line and to the foreground, which mitigates the two halves effect.
- 8. *The sun is present in the photograph that takes attention away (“Sun”).* Some center horizon photographs feature the sun or bright sunlight that distracts from the horizon line. The sun is often located at or near the thirds line, so that it coincides with having a thirds line subject, but this is not always this case. Fig OS20 gives some examples of center horizon photographs featuring the sun.

A total of 82 of the 248 (26.7%) photographs consisted of a reflection across the horizon line. Reflections were compelling enough on their own that no other explanatory pattern was needed alongside them, so we excluded reflection photographs from the subsequent analysis. For the remaining 166 photographs, we tagged each with every applicable compositional element from the above list. The mean and median number of compositional elements exhibited by a center horizon photograph were 2.187 and 2, respectively. The maximum number of compositional elements exhibited by a single center horizon photograph was 4. For each compositional element, we provide in Table 4 the count of center horizon photographs that exhibit that element, as well as the count of center horizon photographs that exhibit *only* that element (we will refer to this as the “exclusive count” of a feature). Exclusive counts for each feature are important to note, as they indicate that for a particular photograph, one compositional element by itself explains the breaking of the center horizon rule. From the table, it appears that leading lines and object crossings are among the most prolific explanatory patterns for breaking the center horizon rule, as they both are commonly exhibited in center horizon photographs, and are the sole explanatory pattern for the rule-break in 4 and 7 of the center horizon photographs, respectively. Sun and busy foregrounds were less so, but also were each the sole justifications for at least some of the center horizon photographs.

We used our features described in Section **Feature description** to assess whether there existed any meaningful differences between center and non-center horizon photographs among each of our nine features. We conducted a two-sided *t*-test between

measurements of each of our 11 features within center horizon photographs vs. 575  
measurements of that feature within non-center horizon photographs. To supplement 576  
our *t*-tests, we constructed kernel density plots and side-by-side boxplots to compare the 577  
two sets of measurements. The plots were used to identify any possible non-linear 578  
differences that the *t*-test would not pick up. 579

Our analysis found no noteworthy differences between center and non-center horizon 580  
photographs among any of our 9 features. For each feature, the p-value of the 581  
corresponding *t*-test did not indicate any significant difference. The kernel density plots 582  
and side-by-side boxplots also did not suggest any differences, linear or non-linear. We 583  
performed a manual inspection of the two sets of photographs and also did not find any 584  
differences of note. We also assessed the proportions of black and white and silhouette 585  
photographs in both center and non-center horizon photographs. 7.83% of center 586  
horizon and 6.76% of non-center horizon photographs were black and white. 18.67% of 587  
center horizon and 18.41% of non-center horizon photographs were silhouettes. These 588  
proportions were very similar for both subcategories. 589

## Subject in the center

We identified a total of 225 high-quality photographs that had their subject placed in 590  
the center. Among them, 105 were placed in the center in the horizontal direction, but 591  
not the vertical direction (“left-right center”). The remaining 120 were placed in the 592  
center in both the horizontal and vertical direction (“true center”). Fig OS21 gives an 593  
example each of left-right center and true center photographs. Both types of center 594  
placement are considered rule-breaks. To identify true center photographs, we used the 595  
following process: 596

1. We first standardized the values of the positions of each photograph to fall 598  
between 0 and 1. It means that, for instance, the center point of any given 599  
photograph would always be represented by (0.5, 0.5), the bottom left corner 600  
would always be represented by (0, 0), and the top right corner by (1, 1). 601
2. Next, we computed the weighted centroid of our subject region. To do this, we 602  
computed the weighted average of the *x* and *y* coordinates of all non-zero pixels in 603  
our saliency map. The weight for each pixel is given by the value of that pixel in 604  
the saliency map divided by the max value among all pixels in the saliency map. 605  
The resulting centroid is then represented in the standardized notation from the 606  
previous step. 607
3. We then computed the Euclidean distance between the center (0.5, 0.5) of the 608  
photograph and the centroid computed in the previous step. 609
4. We then took every photograph with Euclidean distance less than 0.025 as true 610  
center subject photographs. 611

To identify left-right center photographs, we used a very similar approach to the 612  
above. However, instead of computing the Euclidean distance in the third step, we 613  
computed the horizontal distance between the center and the centroid, i.e., the absolute 614  
difference between 0.5 and the *x*-coordinate of the centroid. We then considered every 615  
photograph with a horizontal distance less than 0.025 as left-right center photographs. 616  
To prevent misidentification due to potential measurement errors, we then manually 617  
inspected each photograph that was identified as being either true center or left-right 618  
center, and removed ones that were placed erroneously. 619

The explanatory patterns present were similar between left-right true center 620  
photographs, although they occurred at somewhat different rates. Below we describe 621  
seven explanatory patterns: 622

1. *Symmetry*. Many of the subjects placed in both the left-right and true centers exhibited symmetry. Fig OS22 gives examples of some photographs with centered subjects exhibiting symmetry. While the majority of the exhibited symmetry was from left to right (with a vertical dividing line), there were a few cases of top-bottom symmetry (with a horizontal dividing line), as well as angled symmetry (with a diagonal dividing line). While the majority of cases of symmetry among center subject photographs were quite exact, some photographs exhibited only approximate symmetry.  
623  
624  
625  
626  
627  
628  
629  
630
2. *Circular shaped objects (“Circular”)*. Many of the centered subjects had circular shapes, or had a very circular shaped component. Fig OS23 provides some examples of circular shaped objects. Generally speaking, circular shapes lend themselves well to being placed in the center. Oftentimes, but not always, centered subject photographs containing circular shapes also exhibit symmetry.  
631  
632  
633  
634  
635
3. *Important elements in thirds lines (“Thirds Elements”)*. Since the subject is often the most important compositional element in the photograph, centered subject photographs still often place important elements placed at “thirds intersection points.” Fig OS24 gives some examples of such photographs. The caption for each subfigure describes the important element that falls in the thirds intersection lines.  
636  
637  
638  
639  
640
4. *Gestalt*. Gestalt can be thought of as the principle of “the whole is greater than the sum of its parts” [25]. In other words, in some high-quality photographs, the elements of the photograph are very carefully chosen and highlighted to create an overall “story” to the photograph. Fig OS25 shows examples of centered subject photographs that feature gestalt. In each of these photographs, as well as centered subject photographs featuring gestalt in general, the amount of space on both the left and right side are vital, as both sides contain elements that add to the overall “story” of the photograph. In Fig OS25a, the space on the left is needed to show where the diagonal shadow lines terminate, and the space on the right is required as there needs to be space for the man to stare. In Fig OS25b, the space to the left and right are integral to the story of the photograph. The space on the left serves to make it more clear that the man wearing the orange 4 jersey is running to the left. The space on the right provides room for the other two men to stare. It is clear, for example, that the crouching man is staring at the grass to the right. In Fig OS25c, the space on both the left and right are needed to be able to depict the entire mural in the back. Also, placing the subject in the center tells the story of the person walking from the left, and towards the right. In Fig OS25d, the space on the left makes room for the horseshoe-shaped ring, and the space on the right provides enough room for the cross. The presence of these two objects enhances the impact of the photograph and causes it to be more effective than if only the house itself was depicted. Gestalt was among the most interesting explanatory patterns we found among centered subject photographs.  
641  
642  
643  
644  
645  
646  
647  
648  
649  
650  
651  
652  
653  
654  
655  
656  
657  
658  
659  
660  
661  
662
5. *Frame around the subject (“Frame”)*. Some centered subject photographs featured a framing device around the subject which creates an effect of “frame within a frame” (the outer frame being the photograph itself). Fig OS26 depicts some centered subject photographs with frames around the subject. When such a framing device is present, that frame often acts as the de facto boundaries of the photograph, and thus we would opt to consider the subject’s placement within the framing device rather than the photograph itself. Notably, the frame pictured in a photograph does not have to be an actual frame in the traditional sense, but can be any arrangement that creates a framing-type effect. Frames were also among  
663  
664  
665  
666  
667  
668  
669  
670  
671

**Table 5.** Counts for the center subject patterns.

Pattern	True Center Count	Left Right Count
Symmetry	52	63
Circular	40	19
Thirds Elements	53	25
Gestalt	13	25
Frame	10	8
Leading lines	12	0
Perspective lines	5	16

the most interesting explanatory patterns we found among centered subject photographs.

- 6. *Leading lines.* Leading lines, discussed earlier in Section **Horizon lines**, also played a role in some center subject photographs. Fig OS27 presents some examples of centered subject photographs featuring leading lines. They feature lines, some blatant and others more subtle that lead either towards or away from the subject (i.e., the center of the photograph). When the leading lines lead away, attention is drawn away from the center, making the subject placement more appropriate.
- 7. *Perspective lines.* Perspective lines are leading lines that create a different perspective, and often converge towards the horizon. Fig OS28 presents some examples of left-right center subject photographs that had perspective lines. Most often, the subject in such photographs was a person staring straight towards the camera, and the perspective line was a road or walkway leading inwards toward the top of the photograph. Generally, such photographs also exhibited symmetry, as the person and the perspective line itself can both be divided into two halves.

Table 5 summarizes the distribution of the above compositional elements among both left-right and true center subject photographs. Thirds elements, symmetry, and circular objects were the most commonly found explanatory patterns for true center photographs. The latter two patterns are closely related, as many true center photographs featuring circular objects also exhibited symmetry. Among left-right center photographs, symmetry was by far the most common explanatory pattern. Gestalt and thirds elements both also appeared a considerable amount among left-right center photographs. Notably, perspective lines appeared far more commonly in left-right center than true center photographs, but leading lines that were not perspective lines appeared much more commonly in true center photographs. Unlike in Section **Horizon lines**, we will not provide the counts of features that were exhibited exclusively in a given photographs. In contrast to center horizon photographs, the compositional elements found in center subject photographs generally all had enough explanatory power on their own such that no other element was needed.

Similarly to Section **Horizon lines**, we assessed whether there exists any meaningful differences between center subject and non-center subject photographs in each feature. We performed two separate analyses, one comparing left-right center subject to non-center subject photographs, and one comparing true center subject to non-center subject photographs. To obtain our non-center subject photographs, we took the set of all high-quality photographs and removed every center subject photograph. It is a good approximation of non-center subject photographs, as the vast majority of high-quality photographs contain at least one object that can be considered a subject.

We conducted each of these analyses in the same manner as in Section **Horizon lines**:  
710  
711 using *t*-tests, kernel density plots and side-by-side boxplots to compare the two  
712 populations of each feature, and then performing a manual inspection of the  
713 photographs to identify high-level explanations.  
714

We found no significant linear or non-linear differences between left-right center and  
714 non-center subject photographs. When we compared true center to non-center subject  
715 photographs, we found that on average true center subject photographs had a  
716 significantly higher average *V* value. The *t*-test comparing average *V* between these two  
717 groups yielded a *p*-value of 0.0021. The plots for average *V* also confirmed that true  
718 center subject photographs had a significantly higher average *V*. Most true center  
719 photographs consisted of a subject with monochrome or near-monochrome background.  
720 Of the 115 true center photographs, 30 had strictly monochrome backgrounds and 62  
721 had simple backgrounds that were a blend of a few different colors. Such photographs  
722 usually had very bright backgrounds, resulting in a higher average *V*. In summary,  
723 there were no significant differences among the features in the aggregate between the  
724 center and non-center subject photographs, save for a higher average *V* among true  
725 center subject photographs.  
726

## Conclusion

With the help of statistical methods, we solidify patterns in photography. Our analysis  
728 provided an objective basis for photographers to solidify concepts and ideas that were  
729 traditionally based on intuition and feel. More specifically, we discovered some patterns  
730 that justify the breaking of the following two common photographic rules:  
731

1. *Center horizon photographs*: photographs with a visible horizon should not place  
732 the horizon right in the center of the photograph, and  
733
2. *(center subject photographs)*: photographs containing a subject should not place  
734 the subject in the center of the photograph.  
735

Patterns we discovered for breaking the first rule included reflections, leading lines,  
736 crossing objects, ambiguous lines, implied lines, thirds line subjects, and busy  
737 foregrounds. For the second rule, we identified symmetry, circular shaped objects, thirds  
738 line elements, gestalt, framing, leading lines, and perspective lines. The most interesting  
739 among these patterns were crossing objects and leading lines for center horizon  
740 photographs, and gestalt and framing for center subject photographs. These were all  
741 phenomena that did not naturally come to mind when imagining what justifications  
742 may exist for these specific rule-breaks.  
743

We also devised a statistically interpretable classification model using high-level  
744 image features to discriminate between high-quality and low-quality photographs.  
745 Performing classification ensured that our features were both effective and  
746 discriminative, and established a directional trend for each feature, in terms of being  
747 associated with high or low-quality photographs. With these features, we obtained a  
748 classification error of 21.73%, which is competitive among many state-of-the-art  
749 methods in the literature [12, 14, 22]. These features were used to measure whether the  
750 center horizon and center subject photographs differed from their respective  
751 counterparts. No substantial difference was found for either rule-break, except for the  
752 average *V* value in comparing true center subject photographs to non-centered subject  
753 photographs.  
754

Future work includes extensions to other types of visual arts, such as paintings,  
755 graphics, and digital art. There are many underlying principles that are common to all  
756 these different types of visual arts, and a similar analysis may benefit visual artists in  
757

various crafts. One could also explore other rule-breaks in photography. While the two  
that we analyzed were two of the most common, there are other photography rules that  
could potentially be broken, such as the rule of odds, which states that photographs  
should generally place an odd number of objects.

758  
759  
760  
761

## References

1. Webb J. *Basics Creative Photography 01: Design Principles*. Bloomsbury Publishing; 2017.
2. Lidwell W, Holden K, Butler J. *Universal Principles of Design*. Rockport Publishers; 2003.
3. Ensenberger P. *Focus on Composing Photos: Focus on the Fundamentals*. Focal Press; 2011.
4. Datta R, D J, Li J, Wang JZ. Studying Aesthetics in Photographic Images Using a Computational Approach. 9th European Conference on Computer Vision. 2006; p. 288–301.
5. Ke Y, Tang X, Jing F. The design of high-level features for photo quality assessment. IEEE Computer Society Conference on Computer Vision and Pattern Recognition. 2006; p. 419–426.
6. Luo Y, Tang X. Photo and video quality evaluation: Focusing on the subject. 10th European Conference on Computer Vision. 2008; p. 386–399.
7. Luo W, Wang X, Tang X. Content-based photo quality assessment. IEEE Computer Society Conference on Computer Vision. 2011; p. 2206–2213.
8. Dhar S, Ordonez V, Berg TL. High level describable attributes for predicting aesthetics and interestingness. The 24th IEEE Computer Society Conference on Computer Vision. 2011; p. 1657–1664.
9. Tang X, Luo W, Wang X. Content-Based Photo Quality Assessment. IEEE Transactions on Multimedia. 2013;15:1930–1943.
10. Nishiyama M, Okabe T, Sato I, Sato Y. Aesthetic quality classification of photographs based on color harmony. The 24th IEEE Computer Society Conference on Computer Vision. 2011; p. 33–40.
11. Marchesotti L, Perronnin F, Larlus D, Csurka G. Assessing the aesthetic quality of photographs using generic image descriptors. IEEE International Conference on Computer Vision. 2011; p. 1784–1791.
12. Dong Z, Shen X, Li H, Tian X. Photo quality assessment with DCNN that understands image well. 21st International Conference, MMM. 2015; p. 524–535.
13. Lu X, Lin Z, Jin H, Yang J, Wang JZ. RAPID: rating pictorial aesthetics using deep learning. Proceedings of the ACM International Conference on Multimedia. 2014; p. 457–466.
14. Jin X, Chi J, Peng S, Tian Y, Ye C, Li X. Deep Image Aesthetics Classification using Inception Modules and Fine-tuning Connected Layer. The 8th International Conference on Wireless Communications and Signal Processing. 2016;.

15. Smith AR. Color Gamut Transform Pairs. SIGGRAPH 78 Conference Proceedings. 1978; p. 12–19.
16. Arthur J, Hatt H. The Colorist. D. Van Nostrand Company; 1908.
17. Zhu W, Liang S, Wei Y, Sun J. Saliency Optimization from Robust Background Detection. IEEE Conference on Computer Vision and Pattern Recognition. 2014;.
18. Zhai Y, Mubarak S. Visual Attention Detection in Video Sequences using Spatiotemporal Cues. Proceedings of the 14th ACM International Conference on Multimedia. 2006; p. 815–924.
19. Gonzalez RC, Woods RE. Digital Image Processing. Prentice Hall; 1977.
20. Sharma G. Digital Color Imaging Handbook. CRC Press; 2003.
21. Murray N, Marchesotti L, Perronnin F. AVA: A large-scale database for aesthetic visual analysis. IEEE Conference on Computer Vision and Pattern Recognition. 2012; p. 2408–2415.
22. Tian X, Dong Z, Yang K, Mei T. Query-Dependent Aesthetic Model With Deep Learning for Photo Quality Assessment. IEEE Transactions on Multimedia. 2015;17:2035–2048.
23. McCullagh P, Nelder JA. Generalized Linear Models. 2nd ed. Chapman & Hall; 1989.
24. Breiman L. Random forests. Machine Learning. 2001;45:5–32.
25. Koffka K. Principles of Gestalt Psychology. New York: Harcourt, Brace. 1935;.

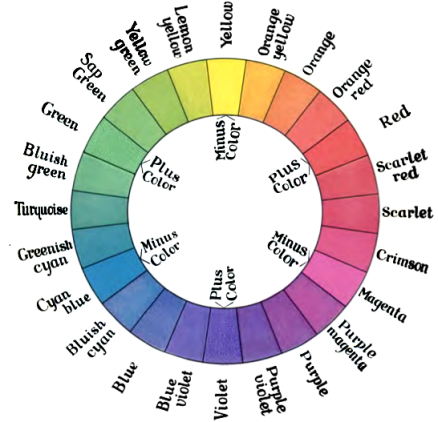
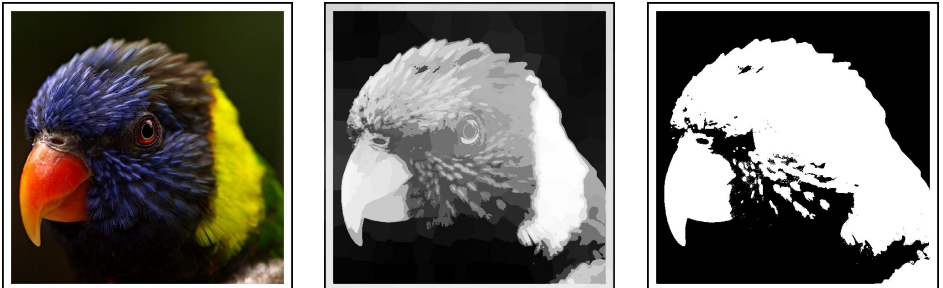


Fig OS1. The color wheel from *The Colorist* (1908).



(a) Original photograph. (b) Saliency Map. (c) Binary Saliency Map.

**Fig OS2.** Saliency map and its binarization.



(a) Clarity measure: 0.993.

(b) Clarity measure: 0.151.

**Fig OS3.** Clarity comparison.



(a) Hue Count: 3.



(b) Hue Count: 9.

**Fig OS4.** Hue count comparison.



**Fig OS5.** A photograph (top left) with 3 of its nearest neighbors.



(a) Percentage Area: 41.3%.



(b) Percentage Area: 26.9%.

**Fig OS6.** Percentage area taken up by subject.



(a) Lighting Contrast: 3.238.



(b) Lighting Contrast: 0.253.

**Fig OS7. Comparison of lighting contrast between subject and background.**



*Top row:*



High-quality photographs. Bottom row: Low-quality photographs.

**Fig OS8. Examples of high and low-quality photographs.**



(a) Lacks a clear subject.



(b) Resulting saliency map.

**Fig OS9.** A fail case of the saliency map.



**Fig OS10.** Silhouettes.



**Fig OS11. Landscapes.**

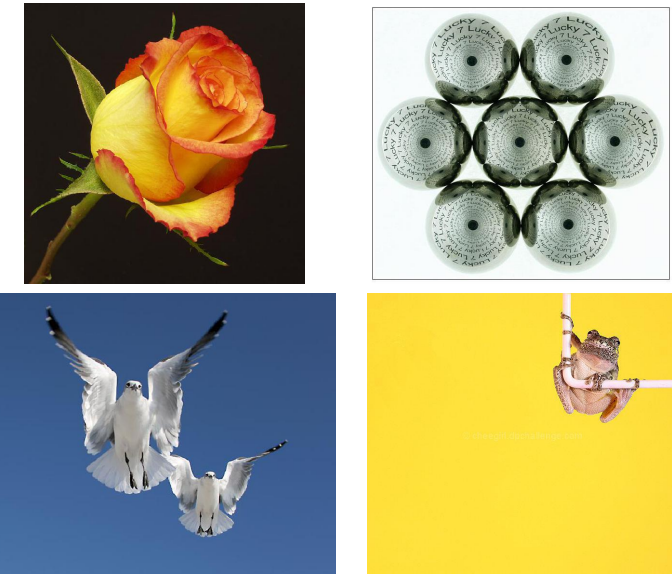


**Fig OS12. Monochrome backgrounds.**



(a) Iceberg reflects over water.



(b) Sky reflects over water.

**Fig OS13. Center horizon photographs featuring reflections.**



(a) The road leads towards the center.



(b) The fence leads into the mountains.



(c) The pavements lead to lighthouse.



(d) The dirt road leads towards the center.

**Fig OS14. Center horizon photographs featuring leading lines.**



(a) The trees on the left cross the center.



(b) The rising wave crosses the center.



(c) Boat and rocks cross the center.



(d) Man and umbrellas cross the center.

**Fig OS15. Center horizon photographs featuring objects crossing the center.**



**Fig OS16. Center horizon photographs with ambiguous horizon lines.**



(a) Where the hill begins on the bottom.



(b) Where the top of the hills meets the sky.



(c) Between the top of the trees and the sky.



(d) Where the dock meets the water.

**Fig OS17. Center horizon photographs with implied lines.**



**Fig OS18. Center horizon photographs with subjects at thirds line intersections.**

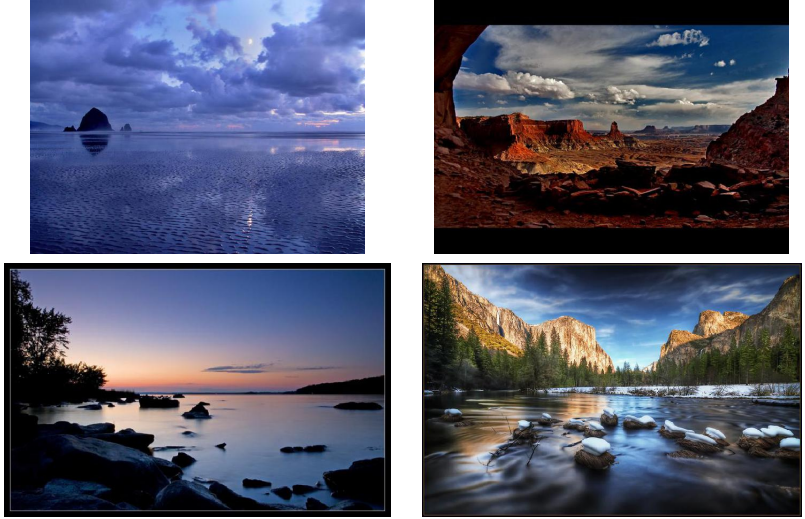


Fig OS19. Center horizon photographs featuring busy foregrounds.

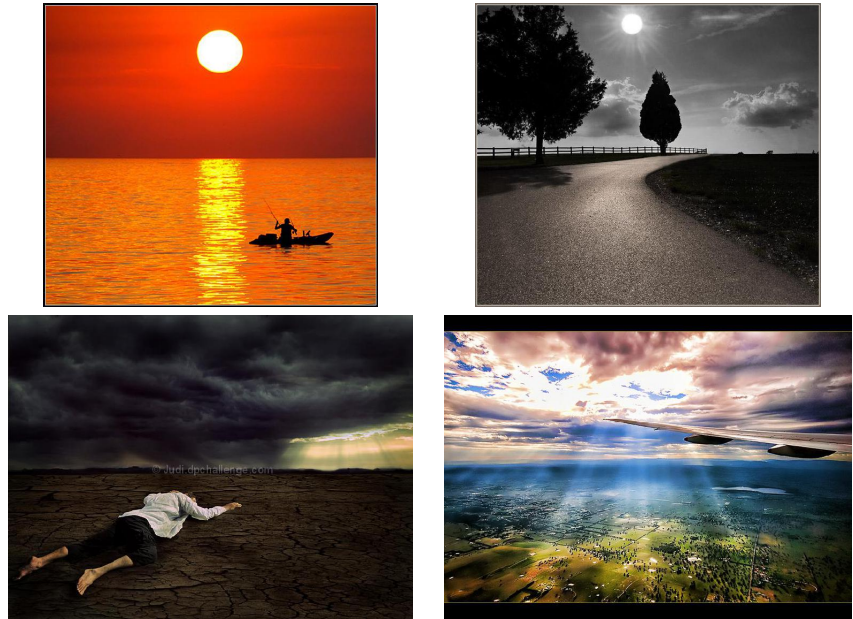
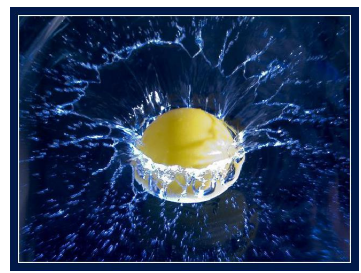


Fig OS20. Center horizon photographs featuring sun or sunlight.



(a) Left-right center subject.

(b) True center subject.

Fig OS21. Left-right vs. true center subject photographs.

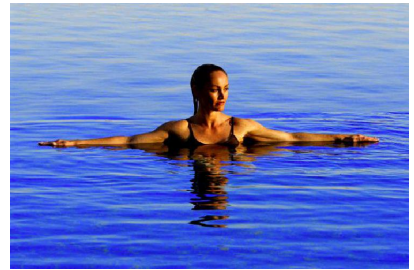


Fig OS22. Center horizon photographs exhibiting symmetry.

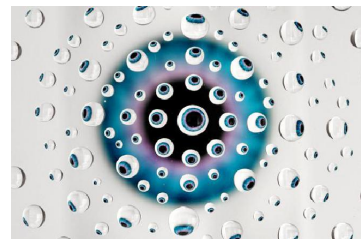
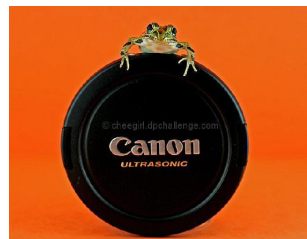


Fig OS23. Center horizon photographs featuring circular shaped objects.



(a) The man's fist.



(b) The horse's front legs and face.



(c) The bird's wings.



(d) The point of reflection at the tip.

**Fig OS24.** Center horizon photographs featuring important elements placed in the thirds lines.



(a)



(b)



(c)



(d)

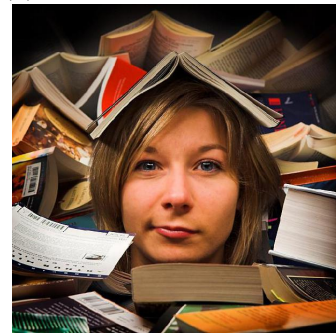
**Fig OS25.** Center horizon photographs featuring gestalt.



(a) The mirror forms a frame.



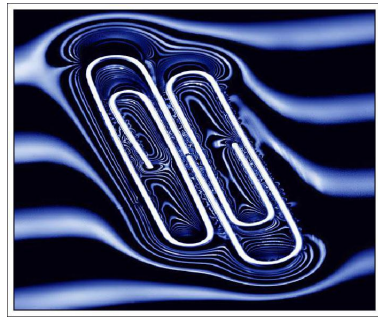
(b) The coils form a frame.



(c) The books form a frame in the center. (d) The black star forms a frame.



Fig OS26. Center horizon photographs featuring frames.



(a) The purple lines are leading lines.



(b) Horizontal lines on the building.

Fig OS27. Center horizon photographs featuring leading lines.



(a) Crosswalk and buildings as perspective lines.



(b) The railroad tracks.



(c) Parallel lines on the house.



(d) The road.

**Fig OS28. Center horizon photographs featuring perspective lines.**